Letter Editors' Suggestion

Enhanced amplitude for superconductivity due to spectrum-wide wave function criticality in quasiperiodic and power-law random hopping models

Xinghai Zhang [1] and Matthew S. Foster [1,2]
[1] *Department of Physics and Astronomy, Rice University, Houston, Texas 77005, USA*
[2] *Rice Center for Quantum Materials, Rice University, Houston, Texas 77005, USA*

(Received 17 April 2022; revised 12 August 2022; accepted 21 October 2022; published 3 November 2022)

We study the interplay of superconductivity and a wide spectrum of critical (multifractal) wave functions ("spectrum-wide quantum criticality," SWQC) in the one-dimensional Aubry-André and power-law random-banded matrix models with attractive interactions, using self-consistent BCS theory. We find that SWQC survives the incorporation of attractive interactions at the Anderson localization transition, whereas the pairing amplitude is maximized near this transition in both models. Our results suggest that SWQC, recently discovered in two-dimensional topological surface-state and nodal superconductor models, can robustly enhance superconductivity.

DOI: 10.1103/PhysRevB.106.L180503

Bulk low-temperature superconductors typically reside in the so-called "dirty limit" $\Delta \ll 1/\tau_{\text{el}}$, where Δ is the spatially averaged order parameter amplitude and $1/\tau_{\text{el}}$ is the elastic scattering rate. As long as the normal state is a good conductor ($\varepsilon_F \tau_{\text{el}} \gg 1$, where ε_F is the Fermi energy), nonmagnetic disorder has a negligible effect on T_c (Anderson's theorem [1,2]). Unconventional superconductors, such as the cuprates and twisted-bilayer graphene [3,4] are effectively two dimensional (2D), however, where arbitrarily weak disorder typically induces Anderson localization of all electronic states [5].

The competition between disorder and superconductivity is responsible for the superconductor-insulator transition [6], which has been a subject of extensive study (see, e.g., Refs. [7–10]). Self-consistent numerical solutions to the Bogoliubov–de Gennes (BdG) equations revealed that strong disorder, which localizes single-particle states, can induce emergent granularity in $\Delta(\mathbf{r})$ [11–13]. This augments phase fluctuations that ultimately destroy superconductivity [11,12,14–16].

A surprising recent development was the realization that superconductivity can sometimes be *enhanced* by random or structured inhomogeneity [14,17–34]. In particular, near the bulk Anderson metal-insulator transition or generally for weak disorder in 2D, the critical rarification (multifractality [35]) of single-particle wave functions induced by quantum interference can enhance interaction matrix elements [22,26,27,36,37]. The multifractal wave functions have larger spatial overlap and stronger state-to-state correlations for states with similar energies ("Chalker scaling" [38–40]), and, therefore, interaction effects are stronger compared to that for extended or localized ones. It was argued that this can boost both the superconducting order parameter amplitude Δ and T_c [13,14,22,26,27,41–43]. Multifractal order parameter modulations have recently been observed in experiments on 2D superconductors [44–48].

In this Letter, we consider a new twist on this theme. In particular, we show that the superconducting amplitude can be strongly enhanced for a system with a wide spectrum of multifractal single-particle wave functions, a phenomenon dubbed "spectrum-wide quantum criticality" (SWQC). SWQC was very recently discovered to arise robustly in 2D surface-state theories with disorder [49–52]. These theories describe surface states of model bulk topological superconductors [37] as well as nodal quasiparticles in dirty 2D d-wave superconductors [51,53]. In these theories, SWQC may be protected by a robust topological mechanism [52].

In this Letter we perform numerical self-consistent BdG calculations on special one-dimensional (1D) systems also known to exhibit SWQC when fine-tuned to the Anderson metal-insulator transition (MIT). (Working in 1D permits us to access much larger system sizes than would be possible in 2D). In particular, we consider the effect of attractive Hubbard interactions for spin-1/2 fermions in the quasiperiodic Aubre-André (AA) and power-law random-banded matrix models. Quasiperiodic systems have recently garnered a surge of interest due to realizations with ultracold atoms [54–64], applications in many-body localization physics [58–60,63,65–67], Hofstadter superconductivity [68,69], and progress in moiré materials [3,4,70–72] with large twist angles [73–80]. The AA model [81,82] is a canonical example of a 1D quasiperiodic system. Although its energy spectrum is well known to possess fractal structure (the Hofstadter butterfly [83,84]), a less-appreciated aspect is the fractality of the corresponding wave functions, which exhibit SWQC at the MIT tuned by the incommensurate potential strength [85,86]. SWQC also occurs in the ensemble of power-law random banded matrices (PRBM) [35,40,87–94].

We find that SWQC survives at a (renormalized) single-particle MIT in the AA and PRBM models with attractive interactions. Our key result is that the superconducting amplitude Δ is enhanced by inhomogeneity relative to the clean case in a wide region around the MIT. The *maximum amplitude* closely tracks the MIT for weak-to-moderate interaction strengths as shown in Figs. 1–3. We also compute the superfluid stiffness D_s for the interacting AA model. We find that D_s is always larger than Δ, except deep in the Anderson insulator

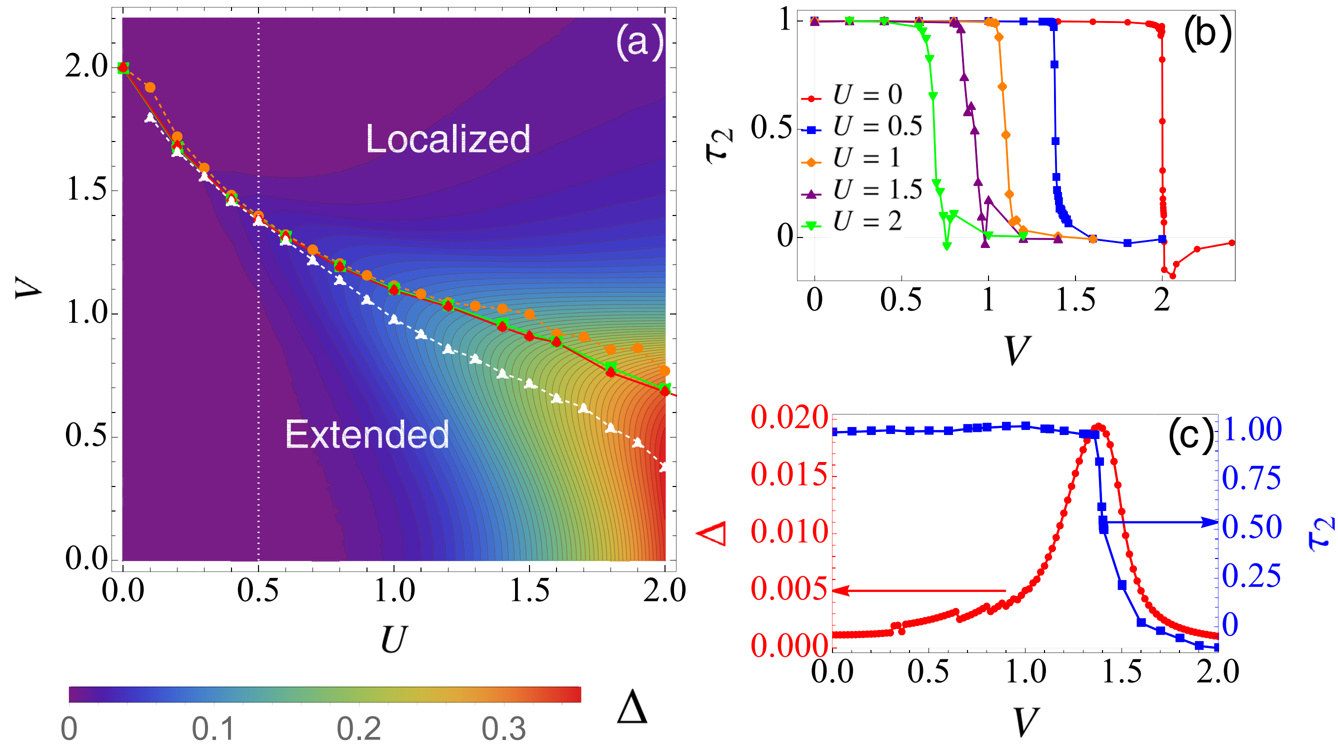

FIG. 1. The enhancement of superconductivity in the AA model with attractive Hubbard interactions, Eq. (1) with $t = 1$. (a) Contour plot of Δ versus attractive interaction strength U and incommensurate potential strength V. The orange ($L_1 = 1597$, $L_2 = 2584$), green ($L_1 = 2584$, $L_2 = 4181$), and red ($L_1 = 4181$, $L_2 = 6765$) curves represent the MIT obtained from scaling of second multifractal dimensions with different system sizes. The strongest enhanced superconductivity with fixed interaction is indicated by the white curve. (b) τ_2-V for different interaction strengths. τ_2 is obtained from the spectrum-averaged inverse participation ratio $\langle P_q\rangle \sim L^{-\tau_q}$ with two system sizes $L_1 = 4181$ and $L_2 = 6765$. The Anderson transition occurs near the sharp drop of τ_2. (c) Δ and τ_2 versus V with $U = 0.5$ [cut indicated by the dotted vertical line in (a)]. Δ peaks around the MIT, where τ_2 drops sharply.

(Fig. 4). Previous studies employing smaller system sizes also demonstrated multifractal enhancement of superconductivity in the interacting AA model [34,42]. In Ref. [42], Δ and D_s were computed, but the location of the MIT and concomitant maximization of Δ were not determined. Our calculations incorporate random Hartree shifts [11,12], an important additional source of quantum interference (Altshuler-Aronov corrections [5]). Our results show that when Anderson localization is prevented in low dimensions (here via fine-tuned potential strengths in special models but as may also occur *generically* in topologically protected 2D systems [49–52]), the rarefied nature of a wide swath of critical single-particle wave functions can strongly boost superconductivity.

Models. The spin-1/2 Aubry-André model with attractive Hubbard interaction is defined via

$$H = -t\sum_{i\sigma}(c^\dagger_{i\sigma}c_{i+1\sigma} + c^\dagger_{i+1\sigma}c_{i\sigma}) + \sum_i (V_i - \mu)n_i - U\sum_i n_{i\uparrow}n_{i\downarrow}, \quad (1)$$

where $c_{i\sigma}$ annihilates a spin-$\sigma \in \{\uparrow, \downarrow\}$ fermion at site i, t is the nearest-neighbor hopping (set to be the energy unit), $V_i = V\cos(2\pi\beta_p i)$ is the incommensurate potential, μ is the chemical potential, U is the strength of attractive on-site interaction, and $n_i = n_{i\uparrow} + n_{i\downarrow}$. We choose $\beta_p \equiv F_{p-1}/F_p$ to approximate the inverse golden ratio, where F_p is the pth Fibonacci number, which is also the system size [86]. The system goes through a spectrum-wide MIT at $V = 2t$ without the interaction term [81,82]. All single-particle wave functions are Anderson localized for $V > 2t$, and all of them are extended for $V < 2t$. All single-particle wave functions are multifractal at the critical point $V = 2t$ [85,86]. The multifractal property of the wave functions can be characterized by the scaling behavior of the inverse participation ratio (IPR) [35], $P_q = \sum_i |\psi_i|^{2q} \propto L^{-\tau_q}$ with L being the system size.

The dimension $\tau_q \equiv D_q(q-1)$, where in 1D $D_q = 1$ ($D_q = 0$) for extended (localized) states, and $0 < D_q < 1$ for critical multifractal wave functions [35]. Wave functions in the extended (localized) phase near the critical point can also show multifractal properties up to the scale of the correlation (localization) length. The multifractality enhancement of superconductivity can occur in a wide region close to the MIT, driven by critical correlations if the coherence length is shorter than the correlation or localization length [22,26].

The Hamiltonian of the spin-1/2 PRBM model with attractive Hubbard interactions is

$$H = \sum_{ij\sigma} \mathrm{H}_{ij}c^\dagger_{i\sigma}c_{j\sigma} - U\sum_i n_{i\uparrow}n_{i\downarrow} - \mu\sum_i n_i, \quad (2)$$

where $\mathrm{H}_{ij} = \mathrm{G}_{ij}|i-j|^{-\alpha}$ with $\hat{\mathrm{G}}$ is a random matrix in the orthogonal class (class AI). Without interactions, the system

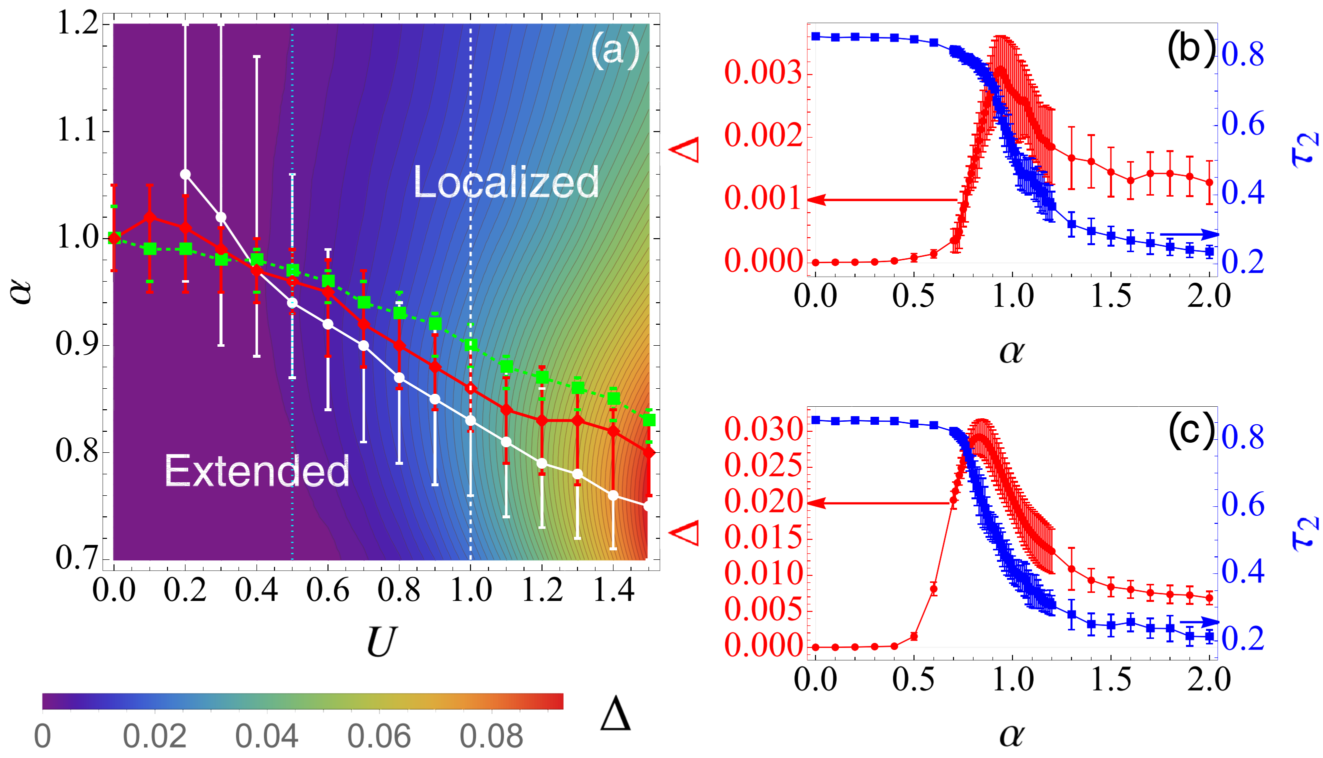

FIG. 2. The enhancement of superconductivity in the PRBM model with attractive Hubbard interactions Eq. (2). (a) Contour plot of Δ versus U and the decay power α, where $\langle\cdots\rangle$ stands for disorder averaging of 20 samples of size $L = 2000$ systems. The MIT occurs at $\alpha = 1$ without interactions, and we use the value of $\tau_2 = -\langle\log(P_2)/\log(L)\rangle$ at $U = 0$ and $\alpha = 1$ as the criteria for the MIT at for nonzero U. The red and green curves represent the MIT obtained by fitting τ_2 using the lowest-lying quasiparticle state and the average of 1% of the low-lying states, respectively. The most enhanced superconductivity is indicated by the white curve. The error bars are obtained from the standard deviation of Δ and τ_2 due to disorder averaging, converted to uncertainty in α. The large error bars reflect the broad enhancement region of superconductivity. (b) and (c) Δ and τ_2 as functions of α for $U = 0.5$ and $U = 1$, respectively [cuts indicated by the dotted vertical lines in (a)]. Δ peaks around the MIT, indicating multifractal enhancement of the order parameter. The wide region of wave-function criticality (indicated by the rather slower decrease in τ_2 compared to the case of the AA model) explains why the maximal enhancement curve [white in (a)] does not follow the MIT curve as well as the case of the AA model.

exhibits SWQC at the MIT with $\alpha = 1$. The system is spectrum-wide extended (localized) when $\alpha < 1$ ($\alpha > 1$) [87].

Phase diagrams. In the mean-field approximation [11–13], the local superconducting order parameter Δ_i and fermion density $\langle n_i\rangle$ satisfy

$$\Delta_i = -U\langle c_{i\downarrow}c_{i\uparrow}\rangle, \quad \langle n_i\rangle = \sum_\sigma \langle c^\dagger_{i\sigma}c_{i\sigma}\rangle. \tag{3}$$

We solve the systems BdG self-consistently [12] with effective chemical potential $\tilde{\mu}_i = \mu + U\langle n_i\rangle/2$. The convergence condition is set so that the average difference of Δ_i and n_i are smaller than 10^{-6} (10^{-7} for small U) [95]. We focus on half-filling with $\mu = -U/2$, but the physics discussed applies to other filling factors since the whole spectrum of single-particle states are multifractal near the MIT.

Figure 1 shows the enhancement of the average order parameter Δ in the BCS-AA model [Eq. (1)]. The spectrum-wide MIT persists with attractive interactions, and the MIT can be characterized by the second multifractal dimension τ_2, averaged over the entire spectrum of quasiparticle states. This shows a sharp drop from 1 to 0 as V increases, indicating the MIT [Fig. 1(b)]. With increasing U, the critical incommensurate potential strength V_c decreases, and the Anderson insulator phase is enlarged (in the mean-field approximation), Fig. 1(a). Δ is enhanced by the multifractal wave functions near the transition, and the maximal Δ for fixed U follows the MIT curve $V_c(U)$ for weak and moderate interactions. When the incommensurate potential strength V is weak, the order parameter is determined by BCS theory with $\Delta \sim \exp(-1/U\nu)$ with ν as the density of states at the Fermi point. As V increases, Δ increases significantly and peaks around the MIT, e.g., $\Delta(V_c)$ is more than ten times larger than $\Delta(V = 0)$ for $U = 0.5$. The order parameter amplitude decreases in the Anderson insulator phase due to the combination of localization and Altshuler-Aronov effects [5,6]. The enhancement ratio $\Delta(V_{\max})/\Delta(V = 0)$ decreases as U increases, and the strongest enhancement curve deviates from the MIT curve at strong interaction.

Apart from inducing SWQC of the wave functions at V_c, the potential in the BCS-AA model additionally generates the interaction-dressed Hofstadter energy spectrum. Band flattening near half-filling plays a role in the enhancement of the order parameter seen here, and the maximum Δ also occurs close to the band flattening point, Figs. 3(a) and 3(b). The density of states is much larger at the band flattening regions, but the average order parameter deviates significantly from

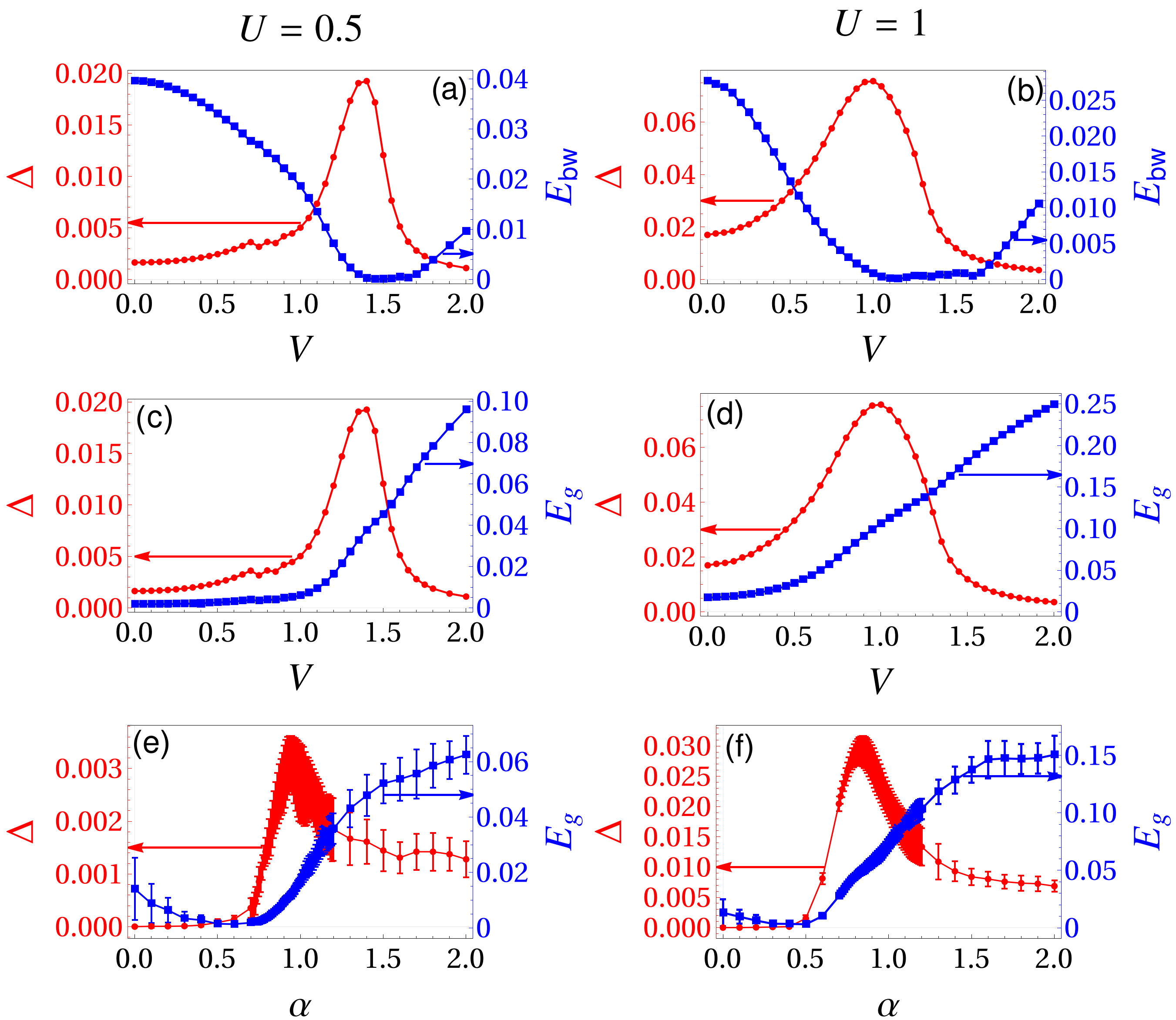

FIG. 3. Superconducting order parameter Δ, and energy bandwidth $E_{\rm bw}$ of the low-lying subband for the BCS-AA model (a) and (b), and single-particle energy gap E_g for the BCS-AA (c) and (d) and BCS-PRBM (e) and (f) models with $U = 0.5$ (the first column) and $U = 1$ (the second column). The order parameter Δ is indicated by the scales on the left axis and red color, whereas $E_{\rm bw}$ and E_g scales appear on the right axis in blue color. (a) Δ and the bandwidth $E_{\rm bw}$ of the lowest-lying subband in the BCS-AA model with $U = 0.5$ (b) Same as (a) except that $U = 1$. The lowest-lying subband becomes almost flat at the MIT, indicating the that the (almost) diverging density of states also plays a role in the enhancement of Δ for the BCS-AA model. (c) Δ and E_g for the BCS-AA model with $U = 0.5$. (d) Same as (c) except that $U = 1$. The order parameter Δ peaks around the MIT, whereas the energy gaps increase monotonically with V, resulting in the deviation of E_g from Δ. (e) Δ and E_g in the BCS-PRBM model with $U = 0.5$. (f) The same as (e) except that $U = 1$. The error bars are from the uncertainty in the disorder averaging. Δ peaks around the MIT and E_g increases with α (except for small α, where E_g has large uncertainty from disorder averaging).

the homogeneous BCS prediction $\Delta \sim \exp(-1/U\nu)$ except for small V ($V < 0.5$ for $U = 0.5$). Multifractal enhancement *without* band flattening is observed in the BCS-PRBM model (described below).

The single-particle wave functions become more and more rarefied with increasing V, resulting in a stronger binding energy between paired electrons occupying the same spatial orbital, and, thus, increasing the spectral gap E_g. In the strong-localization limit, the pairing energy is given by $UP_2(E)$, with $P_2(E)$ as the IPR of the localized state. The energy gap of the BCS-AA model is then given by half the pairing energy $E_g = P_2(E_0)U/2$ [12,95], with E_0 as the energy of the lowest quasiparticle state. Unlike Δ, the gap E_g in our numerics always increases with V, and is much larger than Δ for finite V [Figs. 3(c) and 3(d)]. Thus, whereas the pairing energy of more localized states is larger than extended ones, the average amplitude Δ is suppressed in the insulator by the strong fluctuations of Δ_i in space and the loss of multifractal enhancement. The increasing of E_g into the localization regime is consistent with previous studies indicating that the

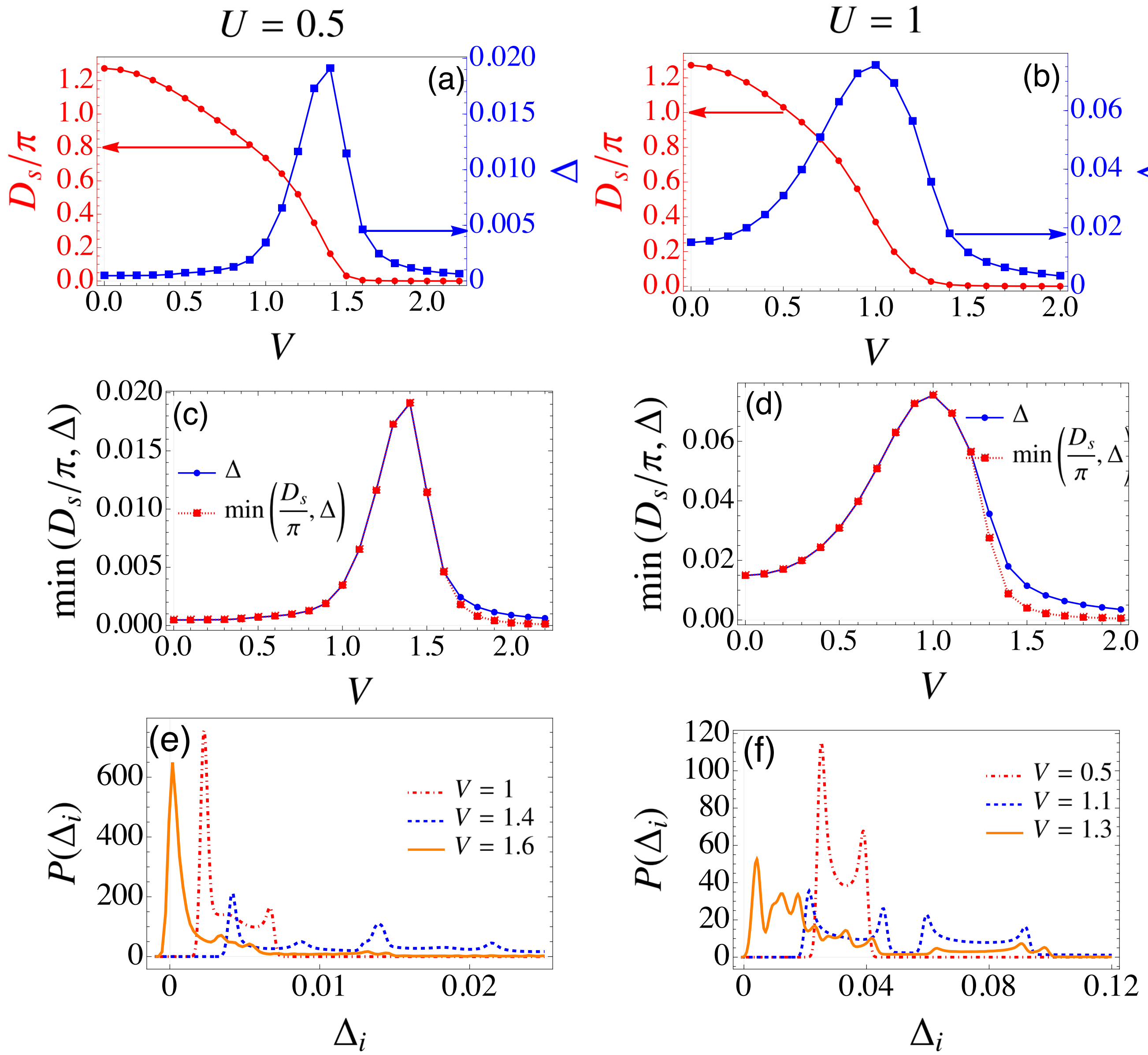

FIG. 4. Superfluid stiffness D_s/π [Eq. (4)], order parameter Δ, and distribution of the local pairing amplitude Δ_i in the BCS-AA model with different interaction strengths $U = 0.5$ (a), (c), and (e) and $U = 1$ (b), (d), and (f). (a) Superfluid stiffness D_s/π (left axis, red color) and order parameter Δ (right axis, blue color) versus incommensurate potential strength V in the BCS-AA model with $U = 0.5$. (b) Same as (a) except $U = 1$. (c) $\min(D_s/\pi, \Delta)$ along with Δ varying with V for $U = 0.5$. (d) Same as (c) except for $U = 1$. In the delocalized phase ($V < V_c \simeq 1.4$ for $U = 0.5$ and $V < V_c \simeq 1.1$ for $U = 1$), $\Delta < D_s/\pi$, and the enhancement of superconductivity is shown by the increasing Δ with V. The phase fluctuations dominate in the localized phase ($V > V_c$), and $D_s/\pi < \Delta$ determines the strength of the superconductivity. The multifractal enhancement of superconductivity persists even incorporating the phase fluctuations. (e) Probability density of local pairing amplitude Δ_i for $U = 0.5$ and different incommensurate potentials. (f) The same as (e) except for $U = 1$. In the delocalized phase and near the MIT, Δ_i peaks around nonzero values, whereas it peaks around 0 in the localized phase. The system size is $L = 2584$ in this figure.

energy gap increases with the inverse of localization length [12,97].

Figure 2 demonstrates the enhancement of Δ in the BCS-PRBM model [Eq. (2)]. Figure 2(a) is a contour plot of Δ as a function of U and the hopping exponent α, near the interaction-dressed MIT. The order parameter Δ takes its largest value close to the MIT curve obtained by fitting τ_2 of the lowest-energy quasiparticle state. The change in τ_2 from the extended phase ($\tau_2 \sim 1$) to the localized phase ($\tau_2 \sim 0$) with α is much slower in the BCS-PRBM model, compared to that in the BCS-AA model, resulting in a much broader critical region. The SWQC wave functions survive in the presence of attractive interactions and pairing, but the τ_2 of the quasiparticle states are affected differently for different states. The lowest-lying quasiparticle states are the best indicator for the MIT and Δ enhancement as these are most involved in pairing. The enhancement always occurs in the critical region, indicated by the drop in τ_2 in Figs. 2(b) and 2(c). The spectral gap E_g in the BCS-PRBM model shows similar behavior as that in the BCS-AA, increasing with α to the localized phase [Figs. 3(e) and 3(f)]. In the localized phase, E_g is also approximately proportional to $P_2(E_0)$ [95]. Different the from the BCS-AA model, there is no significant change in the density of states across the MIT in the BCS-PRBM model, and the critical wave functions are the only factor responsible for enhancing Δ.

Superfluid stiffness. Strong phase fluctuations in low dimensions can demolish superconductivity even if the pairing amplitude remains finite. In a spatially inhomogeneous system, regions with small Δ_i enhance phase fluctuations. The phase rigidity of a superconductor can be described by the superfluid stiffness [98,99]. In a gapped one-dimensional system, the superfluid stiffness is determined by

$$\frac{D_s}{\pi} = \Pi^R_{xx}(q_x = 0, \omega \to 0) - \langle K_x \rangle. \tag{4}$$

Here Π^R_{xx} is the retarded current-current correlation function, and K_x is the kinetic-energy density. The above $q_x = 0$ and $\omega \to 0$ limits give the Drude weight D; it can be shown that $D_s = D$ at zero temperature for gapped systems [98,100]. We employ Eq. (4) to evaluate D_s in the BCS-AA model with s-wave pairing.

Figure 4 shows the superfluid stiffness D_s/π and order parameter Δ in the BCS-AA model. The superfluid stiffness D_s decreases monotonically with increasing incommensurate potential, whereas Δ peaks around MIT, Figs. 4(a) and 4(b). The minimum of D_s/π and Δ determines the strength of the superconductivity. We plot min $(D_s/\pi, \Delta)$ in Figs. 4(c) and 4(d). In the delocalized phase, Δ is much smaller than D_s/π and becomes comparable with D_s/π near the MIT. Only in the localized phase, D_s/π becomes smaller than Δ. The distribution of the local pairing amplitude Δ_i is illustrated in Figs. 4(e) and 4(f). The probability density of Δ_i peaks at nonzero values in the delocalized phase and near the MIT; by contrast, it peaks around 0 in the localized phase. This indicates that the finite average Δ in the localized phase is due to rare regions with large values of Δ_i.

Conclusion. We have shown that the pairing amplitude for superconductivity is enhanced by SWQC in the BCS-AA and -PRBM models. The maximal enhancement tracks the MIT in both models. The enhancement survives phase fluctuations at zero temperature, supported by the superfluid stiffness data for the BCS-AA model. Although true superconductivity does not occur in 1D [101], SWQC also emerges in 2D systems [52]. Strong spatial fluctuations observed in $\Delta(\mathbf{r})$ in the high-T_c cuprate superconductors [102] may realize SWQC for nodal quasiparticles [51].

Generalized AA models have been proposed [103–109] and studied in recent experiments [110–112]. The pairing amplitude enhancement could also be examined in these systems when the Fermi level is tuned close to the mobility edge.

Acknowledgments. We thank F. Evers and N. Trivedi for very useful discussions. This work was supported by the Welch Foundation Grant No. C-1809.

[1] A. A. Abrikosov and L. P. Gorkov, On the theory of superconducting alloys I. The electrodynamics of alloys at absolute zero, Sov. Phys. JETP **8**, 1090 (1959).
[2] P. W. Anderson, Theory of dirty superconductors, J. Phys. Chem. Solids **11**, 26 (1959).
[3] Y. Cao, V. Fatemi, S. Fang *et al.*, Unconventional superconductivity in magic-angle graphene superlattices, Nature (London) **556**, 43 (2018).
[4] E. Y. Andrei and A. H. MacDonald, Graphene bilayers with a twist, Nature Mater. **19**, 1265 (2020).
[5] P. A. Lee and T. V. Ramakrishnan, Disordered electronic systems, Rev. Mod. Phys. **57**, 287 (1985).
[6] M. Ma and P. A. Lee, Localized superconductors, Phys. Rev. B **32**, 5658 (1985).
[7] M. V. Feigel'man, L. B. Ioffe, and M. Mézard, Superconductor-insulator transition and energy localization, Phys. Rev. B **82**, 184534 (2010).
[8] N. Trivedi, Superconductor-insulator transitions: Present status and open questions, in *Conductor-Insulator Quantum Phase Transitions*, edited by V. Dobrosavljević, N. Trivedi, and J. M. Valles, Jr. (Oxford University Press, Oxford, 2012).
[9] A. M. Goldman, Scaling analysis of direct superconductor-insulator transitions in disordered ultrathin films of metals, in *Conductor-Insulator Quantum Phase Transitions*, edited by V. Dobrosavljević, N. Trivedi, and J. M. Valles, Jr. (Oxford University Press, Oxford, 2012).
[10] I. S. Burmistrov, I. V. Gornyi, and A. D. Mirlin, Superconductor-insulator transitions: Phase diagram and magnetoresistance, Phys. Rev. B **92**, 014506 (2015).
[11] A. Ghosal, M. Randeria, and N. Trivedi, Role of Spatial Amplitude Fluctuations in Highly Disordered s-Wave Superconductors, Phys. Rev. Lett. **81**, 3940 (1998).
[12] A. Ghosal, M. Randeria, and N. Trivedi, Inhomogeneous pairing in highly disordered s-wave superconductors, Phys. Rev. B **65**, 014501 (2001).
[13] B. Fan and A. M. García-García, Enhanced phase-coherent multifractal two-dimensional superconductivity, Phys. Rev. B **101**, 104509 (2020).
[14] J. Mayoh and A. M. García-García, Global critical temperature in disordered superconductors with weak multifractality, Phys. Rev. B **92**, 174526 (2015).
[15] Y. Dubi, Y. Meir, and Y. Avishai, Nature of the superconductor-insulator transition in disordered superconductors, Nature (London) **449**, 876 (2007).
[16] A. Erez and Y. Meir, Proposed Measurement of Spatial Correlations at the Berezinski-Kosterlitz-Thouless Transition of Superconducting Thin Films, Phys. Rev. Lett. **111**, 187002 (2013).
[17] E. Arrigoni, E. Fradkin, and S. A. Kivelson, Mechanism of high-temperature superconductivity in a striped Hubbard model, Phys. Rev. B **69**, 214519 (2004).

[18] I. Martin, D. Podolsky, and S. A. Kivelson, Enhancement of superconductivity by local inhomogeneities, Phys. Rev. B **72**, 060502(R) (2005).

[19] S. A. Kivelson and E. Fradkin, How optimal inhomogeneity produces high temperature superconductivity, *Handbook of High-Temperature Superconductivity*, edited by J. R. Schrieffer and J. S. Brooks (Springer, New York, 2007).

[20] K. Aryanpour, E. R. Dagotto, M. Mayr, T. Paiva, W. E. Pickett, and R. T. Scalettar, Effect of inhomogeneity on *s*-wave superconductivity in the attractive Hubbard model, Phys. Rev. B **73**, 104518 (2006).

[21] K. Aryanpour, T. Paiva, W. E. Pickett, and R. T. Scalettar, *s*-wave superconductivity phase diagram in the inhomogeneous two-dimensional attractive Hubbard model, Phys. Rev. B **76**, 184521 (2007).

[22] M. V. Feigel'man, L. B. Ioffe, V. E. Kravtsov, and E. A. Yuzbashyan, Eigenfunction Fractality and Pseudogap State near the Superconductor-Insulator Transition, Phys. Rev. Lett. **98**, 027001 (2007).

[23] Y. Zou, I. Klich, and G. Refael, Effect of inhomogeneous coupling on BCS superconductors, Phys. Rev. B **77**, 144523 (2008).

[24] W.-F. Tsai, H. Yao, A. Läuchli, and S. A. Kivelson, Optimal inhomogeneity for superconductivity: Finite-size studies, Phys. Rev. B **77**, 214502 (2008).

[25] F. Mondaini, T. Paiva, R. R. dos Santos, and R. T. Scalettar, Disordered two-dimensional superconductors: Roles of temperature and interaction strength, Phys. Rev. B **78**, 174519 (2008).

[26] M. V. Feigel'man, L. B. Ioffe, V. E. Kravtsov, and E. Cuevas, Fractal superconductivity near localization threshold, Ann. Phys. (NY) **325**, 1390 (2010).

[27] I. S. Burmistrov, I. V. Gornyi, and A. D. Mirlin, Enhancement of the Critical Temperature of Superconductors by Anderson Localization, Phys. Rev. Lett. **108**, 017002 (2012).

[28] V. Kravtsov, Wonderful life at weak Coulomb interaction: increasing of superconducting/superfluid transition temperature by disorder, J. Phys.: Conf. Ser. **376**, 012003 (2012).

[29] L. Dell'Anna, Enhancement of critical temperatures in disordered bipartite lattices, Phys. Rev. B **88**, 195139 (2013).

[30] R. Mondaini, T. Ying, T. Paiva, and R. T. Scalettar, Determinant quantum Monte Carlo study of the enhancement of *d*-wave pairing by charge inhomogeneity, Phys. Rev. B **86**, 184506 (2012).

[31] J. F. Dodaro and S. A. Kivelson, Generalization of Anderson's theorem for disordered superconductors, Phys. Rev. B **98**, 174503 (2018).

[32] M. N. Gastiasoro and B. M. Andersen, Enhancing superconductivity by disorder, Phys. Rev. B **98**, 184510 (2018).

[33] I. S. Burmistrov, I. V. Gornyi, and A. D. Mirlin, Multifractally-enhanced superconductivity in thin films, Ann. Phys. (NY) **435**, 168499 (2021).

[34] M. Tezuka and A. M. A. M. García-García, Stability of the superfluid state in a disordered one-dimensional ultracold fermionic gas, Phys. Rev. A **82**, 043613 (2010).

[35] F. Evers and A. D. Mirlin, Anderson transitions, Rev. Mod. Phys. **80**, 1355 (2008).

[36] M. S. Foster and E. A. Yuzbashyan, Interaction-Mediated Surface-State Instability in Disordered Three-Dimensional Topological Superconductors with Spin SU(2) Symmetry, Phys. Rev. Lett. **109**, 246801 (2012).

[37] M. S. Foster, H.-Y. Xie, and Y.-Z. Chou, Topological protection, disorder, and interactions: Survival at the surface of 3D topological superconductors, Phys. Rev. B **89**, 155140 (2014).

[38] J. T. Chalker and G. J. Daniell, Scaling, Diffusion, and the Integer Quantized Hall Effect, Phys. Rev. Lett. **61**, 593 (1988).

[39] J. T. Chalker, Scaling and eigenfunction correlations near a mobility edge, Physica A **167**, 253 (1990).

[40] E. Cuevas and V. E. Kravtsov, Two-eigenfunction correlation in a multifractal metal and insulator, Phys. Rev. B **76**, 235119 (2007).

[41] B. Fan and A. M. García-García, Superconductivity at the three-dimensional Anderson metal-insulator transition, Phys. Rev. B **102**, 184507 (2020).

[42] Z. Fan, G.-W. Chern, and S.-Z. Lin, Enhanced superconductivity in quasiperiodic crystals, Phys. Rev. Res. **3**, 023195 (2021).

[43] M. Stosiek, F. Evers, and I. S. Burmistrov, Multifractal correlations of the local density of states in dirty superconducting films, Phys. Rev. Res. **3**, L042016 (2021).

[44] K. Zhao, H. Lin, X. Xiao, W. Huang, W. Yao, M. Yan, Y. Xing, Q. Zhang, Z.-X. Li, S. Hoshino, J. Wang, S. Zhou, L. Gu, M. S. Bahramy, H. Yao, N. Nagaosa, Q.-K. Xue, K. T. Law, X. Chen, and S.-H. Ji, Disorder-induced multifractal superconductivity in monolayer niobium dichalcogenides, Nat. Phys. **15**, 904 (2019).

[45] C. Rubio-Verdú, A. M. García-García, H. Ryu, D.-J. Choi, J. Zaldívar, S. Tang, B. Fan, Z.-X. Shen, S.-K. Mo, J. I. Pascual, and M. M. Ugeda, Visualization of multifractal superconductivity in a two-dimensional transition metal dichalcogenide in the weak-disorder regime, Nano Lett. **20**, 5111 (2020).

[46] C. Carbillet, V. Cherkez, M. A. Skvortsov, M. V. Feigel'man, F. Debontridder, L. B. Ioffe, V. S. Stolyarov, K. Ilin, M. Siegel, D. Roditchev, T. Cren, and C. Brun, Spectroscopic evidence for strong correlations between local superconducting gap and local Altshuler-Aronov density of states suppression in ultrathin NbN films, Phys. Rev. B **102**, 024504 (2020).

[47] A. Ślebarski, M. Fijałkowski, P. Zajdel, M. M. Maśka, J. Deniszczyk, M. Zubko, O. Pavlosiuk, K. Sasmal, and M. B. Maple, Enhancing superconductivity of $Y_5Rh_6Sn_{18}$ by atomic disorder, Phys. Rev. B **102**, 054514 (2020).

[48] A. Ślebarski, M. Fijałkowski, M. M. Maśka, J. Deniszczyk, P. Zajdel, B. Trump, and A. Yakovenko, Enhancing superconductivity of $Lu_5Rh_6Sn_{18}$ by atomic disorder, Phys. Rev. B **103**, 155133 (2021).

[49] S. A. A. Ghorashi, Y. Liao, and M. S. Foster, Critical Percolation without Fine-Tuning on the Surface of a Topological Superconductor, Phys. Rev. Lett. **121**, 016802 (2018).

[50] B. Sbierski, J. F. Karcher, and M. S. Foster, Spectrum-Wide Quantum Criticality at the Surface of Class AIII Topological Phases: An "Energy Stack" of Integer Quantum Hall Plateau Transitions, Phys. Rev. X **10**, 021025 (2020).

[51] S. A. A. Ghorashi, J. F. Karcher, S. M. Davis, and M. S. Foster, Criticality across the energy spectrum from random artificial gravitational lensing in two-dimensional Dirac superconductors, Phys. Rev. B **101**, 214521 (2020).

[52] J. F. Karcher and M. S. Foster, How spectrum-wide quantum criticality protects surface states of topological superconductors from Anderson localization: Quantum Hall plateau

transitions (almost) all the way down, Ann. Phys. (NY) **435**, 168439 (2021).

[53] A. Altland, B. D. Simons, and M. R. Zirnbauer, Theories of low-energy quasi-particle states in disordered d-wave superconductors, Phys. Rep. **359**, 283 (2002).

[54] L. Guidoni, C. Triché, P. Verkerk, and G. Grynberg, Quasiperiodic Optical Lattices, Phys. Rev. Lett. **79**, 3363 (1997).

[55] G. Roati, C. D'Errico, L. Fallani *et al.*, Anderson localization of a non-interacting Bose-Einstein condensate, Nature (London) **453**, 895 (2008).

[56] L. Sanchez-Palencia and M. Lewenstein, Disordered quantum gases under control, Nat. Phys. **6**, 87 (2010).

[57] B. Deissler, M. Zaccanti, G. Roati *et al.*, Delocalization of a disordered bosonic system by repulsive interactions, Nat. Phys. **6**, 354 (2010).

[58] M. Schreiber, S. S. Hodgman, P. Bordia, H. P. Lüschen, M. H. Fischer, R. Vosk, E. Altman, U. Schneider, and I. Bloch, Observation of many-body localization of interacting fermions in a quasirandom optical lattice, Science **349**, 842 (2015).

[59] P. Bordia, H. P. Lüschen, S. S. Hodgman, M. Schreiber, I. Bloch, and U. Schneider, Coupling Identical One-Dimensional Many-Body Localized Systems, Phys. Rev. Lett. **116**, 140401 (2016).

[60] P. Bordia, H. Lüschen, S. Scherg, S. Gopalakrishnan, M. Knap, U. Schneider, and I. Bloch, Probing Slow Relaxation and Many-Body Localization in Two-Dimensional Quasiperiodic Systems, Phys. Rev. X **7**, 041047 (2017).

[61] K. Viebahn, M. Sbroscia, E. Carter, J.-C. Yu, and U. Schneider, Matter-Wave Diffraction from a Quasicrystalline Optical Lattice, Phys. Rev. Lett. **122**, 110404 (2019).

[62] A. Szabó and U. Schneider, Mixed spectra and partially extended states in a two-dimensional quasiperiodic model, Phys. Rev. B **101**, 014205 (2020).

[63] M. Sbroscia, K. Viebahn, E. Carter, J.-C. Yu, A. Gaunt, and U. Schneider, Observing Localization in a 2D Quasicrystalline Optical Lattice, Phys. Rev. Lett. **125**, 200604 (2020).

[64] R. Gautier, H. Yao, and L. Sanchez-Palencia, Strongly Interacting Bosons in a Two-Dimensional Quasicrystal Lattice, Phys. Rev. Lett. **126**, 110401 (2021).

[65] S. Iyer, V. Oganesyan, G. Refael, and D. A. Huse, Many-body localization in a quasiperiodic system, Phys. Rev. B **87**, 134202 (2013).

[66] K. Agarwal, E. Altman, E. Demler, S. Gopalakrishnan, D. A. Huse, and M. Knap, Rare-region effects and dynamics near the many-body localization transition, Ann. Phys. (NY) **529**, 1600326 (2017).

[67] D. A. Abanin, E. Altman, I. Bloch, and M. Serbyn, *Colloquium*: Many-body localization, thermalization, and entanglement, Rev. Mod. Phys. **91**, 021001 (2019).

[68] D. Shaffer, J. Wang, and L. H. Santos, Theory of Hofstadter superconductors, Phys. Rev. B **104**, 184501 (2021).

[69] D. Shaffer, J. Wang, and L. H. Santos, Unconventional Self-Similar Hofstadter Superconductivity from Repulsive Interactions, arXiv:2204.13116.

[70] R. Bistritzer and A. H. MacDonald, Moiré bands in twisted double-layer graphene, Proc. Natl. Acad. Sci. USA **108**, 12233 (2011).

[71] J. M. B. Lopes dos Santos, N. M. R. Peres, and A. H. Castro Neto, Graphene Bilayer with a Twist: Electronic Structure, Phys. Rev. Lett. **99**, 256802 (2007).

[72] Y. Cao, V. Fatemi, A. Demir *et al.*, Correlated insulator behaviour at half-filling in magic-angle graphene superlattices, Nature (London) **556**, 80 (2018).

[73] P. Moon and M. Koshino, Optical absorption in twisted bilayer graphene, Phys. Rev. B **87**, 205404 (2013).

[74] S. Spurrier and N. R. Cooper, Theory of quantum oscillations in quasicrystals: Quantizing spiral Fermi surfaces, Phys. Rev. B **100**, 081405(R) (2019).

[75] H. K. Pal, S. Spitz, and M. Kindermann, Emergent Geometric Frustration and Flat Band in Moiré Bilayer Graphene, Phys. Rev. Lett. **123**, 186402 (2019).

[76] M. Mirzakhani, F. M. Peeters, and M. Zarenia, Circular quantum dots in twisted bilayer graphene, Phys. Rev. B **101**, 075413 (2020).

[77] J. Bucko and F. Herman, Large twisting angles in bilayer graphene moiré quantum dot structures, Phys. Rev. B **103**, 075116 (2021).

[78] W. Yao, E. Wang, C. Bao, Y. Zhang, K. Zhang, K. Bao, C. K. Chan, C. Chen, J. Avila, M. C. Asensio, J. Zhu, and S. Zhou, Quasicrystalline 30° twisted bilayer graphene as an incommensurate superlattice with strong interlayer coupling, Proc. Natl. Acad. Sci. USA **115**, 6928 (2018).

[79] S. J. Ahn, P. Moon, T.-H. Kim, H.-W. Kim, H.-C. Shin, E. H. Kim, H. W. Cha, S.-J. Kahng, P. Kim, M. Koshino, Y.-W. Son, C.-W. Yang, and J. R. Ahn, Dirac electrons in a dodecagonalgraphene quasicrystal, Science **361**, 782 (2018).

[80] F. C. Bocquet, Y.-R. Lin, M. Franke, N. Samiseresht, S. Parhizkar, S. Soubatch, T.-L. Lee, C. Kumpf, and F. S. Tautz, Surfactant-Mediated Epitaxial Growth of Single-Layer Graphene in an Unconventional Orientation on SiC, Phys. Rev. Lett. **125**, 106102 (2020).

[81] S. Aubry and G. André, Analyticity breaking and Anderson localization in incommensurate lattices, Ann. Isr. Phys. Soc. **3**, 133 (1980).

[82] J. B. Sokoloff, Unusual band structure, wave functions and electrical conductance in crystals with incommensurate periodic potentials, Phys. Rep. **126**, 189 (1985).

[83] D. R. Hofstadter, Energy levels and wave functions of Bloch electrons in rational and irrational magnetic fields, Phys. Rev. B **14**, 2239 (1976).

[84] C. Tang and M. Kohmoto, Global scaling properties of the spectrum for a quasiperiodic Schrödinger equation, Phys. Rev. B **34**, 2041 (1986).

[85] S. N. Evangelou, Multi-fractal spectra and wavefunctions of one-dimensional quasi-crystals, J. Phys. C: Solid State Phys. **20**, L295 (1987).

[86] A. P. Siebesma and L. Pietronero, Multifractal properties of wave functions for one-dimensional systems with an incommensurate potential, Europhys. Lett. **4**, 597 (1987).

[87] A. D. Mirlin, Statistics of energy levels and eigenfunctions in disordered systems, Phys. Rep. **326**, 259 (2000).

[88] A. D. Mirlin, Y. V. Fyodorov, F.-M. Dittes, J. Quezada, and T. H. Seligman, Transition from localized to extended eigenstates in the ensemble of power-law random banded matrices, Phys. Rev. E **54**, 3221 (1996).

[89] V. E. Kravtsov and K. A. Muttalib, New Class of Random Matrix Ensembles with Multifractal Eigenvectors, Phys. Rev. Lett. **79**, 1913 (1997).

[90] F. Evers and A. D. Mirlin, Fluctuations of the Inverse Participation Ratio at the Anderson Transition, Phys. Rev. Lett. **84**, 3690 (2000).
[91] A. D. Mirlin and F. Evers, Multifractality and critical fluctuations at the Anderson transition, Phys. Rev. B **62**, 7920 (2000).
[92] V. E. Kravtsov, A. Ossipov, O. M. Yevtushenko, and E. Cuevas, Dynamical scaling for critical states: Validity of Chalker's ansatz for strong fractality, Phys. Rev. B **82**, 161102(R) (2010).
[93] V. E. Kravtsov, O. M. Yevtushenko, P. Snajberk, and E. Cuevas, Lévy flights and multifractality in quantum critical diffusion and in classical random walks on fractals, Phys. Rev. E **86**, 021136 (2012).
[94] V. E. Kravtsov, I. M. Khaymovich, E. Cuevas, and M. Amini, A random matrix model with localization and ergodic transitions, New J. Phys. **17**, 122002 (2015).
[95] See Supplemental Material at https://link.aps.org/supplemental/10.1103/PhysRevB.106.L180503 instructions for convergence condition, scaling of the IPR with system size, relation between E_g and $P_2(E_0)$, more information on the multifractal properties of the wave functions, Chalker scaling, and which includes Ref. [96].
[96] T. C. Halsey, M. H. Jensen, L. P. Kadanoff, I. Procaccia, and B. I. Shraiman, Fractal measures and their singularities: The characterization of strange sets, Phys. Rev. A **33**, 1141 (1986).
[97] K. Bouadim, Y. L. Loh, M. Randeria, and N. Trivedi, Single- and two-particle energy gaps across the disorder-driven superconductor-insulator transition, Nat. Phys. **7**, 884 (2011).
[98] D. J. Scalapino, S. R. White, and S. Zhang, Insulator, metal, or superconductor: The criteria, Phys. Rev. B **47**, 7995 (1993).
[99] N. Trivedi, R. T. Scalettar, and M. Randeria, Superconductor-insulator transition in a disordered electronic system, Phys. Rev. B **54**, R3756(R) (1996).
[100] T. Giamarchi and B. S. Shastry, Persistent currents in a one-dimensional ring for a disordered Hubbard model, Phys. Rev. B **51**, 10915 (1995).
[101] T. Giamarchi, *Quantum Physics in One Dimension* (Clarendon Press, Oxford, 2003).
[102] For a review, see, e.g., K. Fujita, A. R. Schmidt, E.-A. Kim, M. J. Lawler, H. Eisaki, S. Uchida, D.-H. Lee, and J. C. Davis, Spectroscopic imaging STM studies of electronic structure in both the superconducting and pseudogap phases of underdoped cuprates, in *Conductor-Insulator Quantum Phase Transitions*, edited by V. Dobrosavljević, N. Trivedi, and J. M. Valles, Jr. (Oxford University Press, Oxford, 2012).
[103] C. M. Soukoulis and E. N. Economou, Localization in One-Dimensional Lattices in the Presence of Incommensurate Potentials, Phys. Rev. Lett. **48**, 1043 (1982).
[104] S. Das Sarma, S. He, and X. C. Xie, Mobility Edge in a Model One-Dimensional Potential, Phys. Rev. Lett. **61**, 2144 (1988).
[105] J. Biddle and S. Das Sarma, Predicted Mobility Edges in One-Dimensional Incommensurate Optical Lattices: An Exactly Solvable Model of Anderson Localization, Phys. Rev. Lett. **104**, 070601 (2010).
[106] S. Ganeshan, J. H. Pixley, and S. Das Sarma, Nearest Neighbor Tight Binding Models with an Exact Mobility Edge in One Dimension, Phys. Rev. Lett. **114**, 146601 (2015).
[107] X. Li, X. Li, and S. Das Sarma, Mobility edges in one-dimensional bichromatic incommensurate potentials, Phys. Rev. B **96**, 085119 (2017).
[108] H. Yao, A. Khoudli, L. Bresque, and L. Sanchez-Palencia, Critical Behavior and Fractality in Shallow One-Dimensional Quasiperiodic Potentials, Phys. Rev. Lett. **123**, 070405 (2019).
[109] H. Yao, T. Giamarchi, and L. Sanchez-Palencia, Lieb-Liniger Bosons in a Shallow Quasiperiodic Potential: Bose Glass Phase and Fractal Mott Lobes, Phys. Rev. Lett. **125**, 060401 (2020).
[110] H. P. Lüschen, S. Scherg, T. Kohlert, M. Schreiber, P. Bordia, X. Li, S. Das Sarma, and I. Bloch, Single-Particle Mobility Edge in a One-Dimensional Quasiperiodic Optical Lattice, Phys. Rev. Lett. **120**, 160404 (2018).
[111] T. Kohlert, S. Scherg, X. Li, H. P. Lüschen, S. Das Sarma, I. Bloch, and M. Aidelsburger, Observation of Many-Body Localization in a One-Dimensional System with a Single-Particle Mobility Edge, Phys. Rev. Lett. **122**, 170403 (2019).
[112] F. A. An, K. Padavić, E. J. Meier, S. Hegde, S. Ganeshan, J. H. Pixley, S. Vishveshwara, and B. Gadway, Interactions and Mobility Edges: Observing the Generalized Aubry-André Model, Phys. Rev. Lett. **126**, 040603 (2021).